ChemComm

Accepted Manuscript

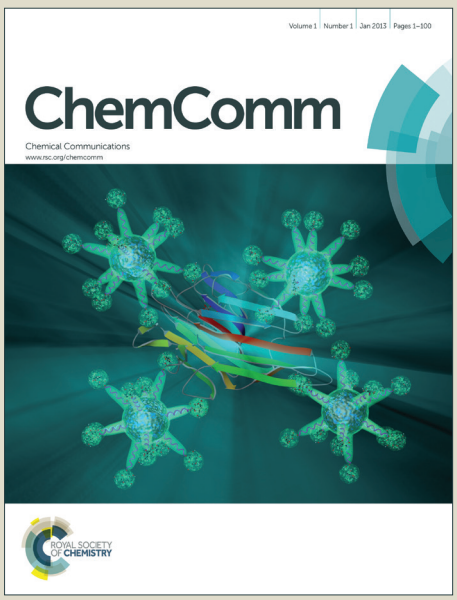

ROYAL SOCIETY OF CHEMISTRY

www.rsc.org/chemcomm

Cite this: DOI: 10.1039/c0xx00000x

www.rsc.org/xxxxxx

COMMUNICATION

Synergistic dual-targeting hydrogel improve targeting and anticancer effect of Taxol *in vitro* and *in Vivo*

Chang Shu,[a] Ruixin Li,[a] Yajun Yin,[a] Deyan Yin,[c] Yueqing Gu,[c] Li Ding*[b] and Wenying Zhong*[a]

Received (in XXX, XXX) Xth XXXXXXXXX 20XX, Accepted Xth XXXXXXXXX 20XX

DOI: 10.1039/b000000x

A synergistic dual-targeting molecular self-assembly hydrogel was designed by estrone (Et) and Arg-Gly-Asp (RGD) peptide to enhance targeting delivery and anticancer effect of Taxol for real-time visualization research *in vitro* and *in vivo*.

The preparation of drug delivery with a multifunctional structure at nanoscale level is an interesting area of medicine science.[1-3] Self-assembly in which engineered molecules as building blocks are gathered by non-covalent or covalent interactions to form nano-delivery, such as particles, fibers and tubules, is an approach to achieve this goal.[4-7] One of potential applications of the molecular self-assemblies is recognized in the drug delivery field, because they will degrade back into individual monomers that can be broken down by the *in vivo* environment.[8, 9] To be an effective and perfect drug delivery, molecular self-assemblies should have several characteristics: 1) High functionality to conjugate multiple therapeutic agents and to have effective interaction with target sites;[10] 2) Biocompatibility and stability in biological systems; 3) Ability to cross different barriers, especially normal cells and perinuclear membrane, in the body;[11] 4) Release therapeutic agents and degrade to biocompatible materials in destination tissues.[12]

As for cancer treatment there are many approaches in targeting pathway. Active targeting is not only limited to hyperproliferative tumor tissues but also involves the ligand-receptor or antigen-antibody mediated endocytosis pathway based on molecular recognition.[13] Cell surface biomolecules, such as estrogen receptors and integrin $\alpha_v\beta_3$, are highly overexpressed in breast cancer and involved in invasion, metastasis and angiogenesis.[14] The overexpression of estrogen receptor (ER) on cancer cells makes them attractive specific-targets for drug delivery.[15] Although estrone could enhance targeting effect, the presence of receptor-targeting moiety would limit the enhanced uptake of drugs due to the estrone receptor saturation.[16] Considering the fact that an ideal targeting drug delivery should not only selectively makes them attractive specific-targets for drug delivery. Although estrone could enhance targeting effect, the presence of receptor-targeting moiety would limit the enhanced uptake of deliver drug to targeted tumor site but also elevate the penetration into the cancer cells with high efficacy, the synergistic anticancer effect drug delivery need to be designed.[17] RGD peptide, which has high affinity for $\alpha_v\beta_3$ integrin, has made important contribution in the fields of targeted drug delivery research. Interaction sites between RGD peptide and integrin $\alpha_v\beta_3$ have been studied extensively, and RGD-containing peptides have been widely used to deliver various kinds of cargos.[18] Having these ideas in mind, we designed the hydrogel drug delivery that consists of (1) estron and RGD peptide as dual targeting moiety, (2) Taxol as an anticancer drug and (3) self-assemble peptide hydrogel as nanoscale carrier will be exceptionally effective for treatment of breast malignance (Fig.1).

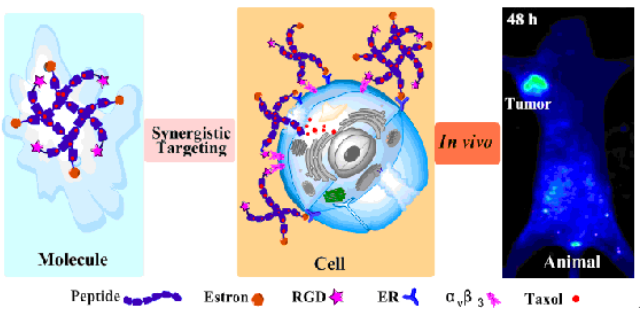

Fig.1 Schematic illustration of the synergistic dual-targeting process of the Et-peptide-Taxol hydrogel *in vitro* and *in vivo*

After the successful synthesis of the Et-peptide-Taxol, its self-assembly ability was evaluated by the treatment with glutathione (GSH).[19] Et-peptide-Taxol was highly soluble in the phosphate buffer saline (PBS) solution (pH = 7.4). The formation of translucent hydrogel (Fig.S-1A) is observed after incubation of the above solution within 10 min at room temperature. The

[a] *Department of Analytical Chemistry, China Pharmaceutical University, Nanjing, 211198, PR China. E-mail: wyzhong@cpu.edu.cn.*
[b] *Department of Pharmaceutical Analysis, China Pharmaceutical University, Nanjing, 210009, PR China. E-mail: dinglihg@sina.com*
[c] *Department of Biomedical Engineering, China Pharmaceutical University, Nanjing, 210009, P.R. China*

† Electronic Supplementary Information (ESI) available: (I) Methods and characterization; (II) Confocal images of MCF-7 cells after incubation with hydrogels for 4 h. (III) Histological analysis of vital organs (heart, liver, spleen, lung, kidney and tumor) treated with Et-peptide-Taxol hydrogel.
See DOI: 10.1039/b000000x/

minimum concentration needed for gelation (MCG) is about 0.8 wt% in PBS solution. The Transmission electron microscopy (TEM) image (Fig.S-1B) reveals the hydrogel self-assembled into short nanofibers with width of 20 nm, in addition to particle aggregates. The nanofibers appear to stretch out of the amorphous area, suggesting that the nanofibers grow from the selfassembly process. Moreover its scanning electron micrograph (SEM) image shows filamentary microstructures (Fig.S-1C). Rheology is used to examine hydrogel viscoelastic properties. The Et-peptide-Taxol hydrogel behaves viscoelastic properties of solid-like materials because the storage moduli (G′) are significantly higher than loss moduli (G″) (Fig.S-3).[20] The hydrogel also exhibits weak frequency dependence in dynamic frequency sweep (Fig.S-3B). These results indicate that Et-peptide-Taxol is an effective hydrogel and it has an excellent self-assembly ability. Zeta potential is −44.7±2.5 mV for Et-peptide-Taxol hydrogel (0.1μg/ml). The negative charge benefits the stability of drug delivery and transportation under biologically relevant conditions inhabiting some undesirable side effects such as thrombosis, embolization and hemolysis *in vivo*.[21]

The Taxol molecule is released from hydrogels by the ester bond hydrolysis in PBS solutions. The release behavior exhibits a sustained release mechanism within 24 h at physiological temperature of 37°C (Fig.2A). There is no burst releases of Taxol, and released Taxol at a constant rate of about 2.377, 4.109 and 6.929 μg/mL per hour throughout the entire measurement period of 24 hours. According to the empirical Ritger-Peppas [22] equation, the rate constant values k are approximately 0.008 (r=0.9980), 0.011(r=0.9983), and 0.014(r=0.9987) for 1.0%, 1.2%, and 1.5% hydrogels, respectively, indicate that the releasing rate of Taxol increased with increasing the content of hydrogels.[23] The exponential factor (n) has been evaluated by fitting the experimental data in order to determine the mechanism involved in the process. The values of n are 0.8883, 0.9126, and 0.9857, for 1.0%, 1.2%, and 1.5% hydrogels, respectively. The values of n obtained between 0.5 and 1 indicate the anomalous nature of drug release to which both diffusion and relaxation processes contribute.[24] The maximum concentration reached at the end of the release process, which can be related to the amount of drug retained into the mesophase due to specific interactions. These results confirm that the release of Taxol molecules trapped in the nanogels obeys to two correlated processes within the delivery matrix. One is a diffusion controlled delivery mechanism. The other is a chemically controlled event related to the breakage of coordinate ester bonds between the drug and the peptide chains.

The cytotoxicity of hydrogel was evaluated with MTT assays (Fig.2B). It could be concluded that free Taxol, Et-peptide-Taxol and Et-peptide-Taxol hydrogel could inhibit the growth of MCF-7 cells in a concentration-dependent manner. Compared with free Taxol, Et-peptide-Taxol and its hydrogel exhibit stronger inhibition effect to the proliferation of MCF-7 cells at various concentrations. But the Et-peptide and its hydrogel without Taxol show no obvious toxicity to the cells. The IC_{50} values of Taxol, Et-peptide-Taxol and Et-peptide-Taxol hydrogel are 38.5±3.12 nM, 16.4±1.67 nM and 14.4±2.93 nM, respectively. The IC_{50} values of most of Taxol derivatives are within the range of 10 to 100 nM,[25] indicating that the modification of Taxol have not reduced the activity of Taxol dramatically. *In vitro* assay demonstrate that the dual-targeting hydrogel led to the most significant improvement in anticancer effect of MCF-7 cells. These indicate that anti-proliferative effect of the drug-loaded hydrogel is markedly elevated by the dual-modification with estrone and RGD peptide.

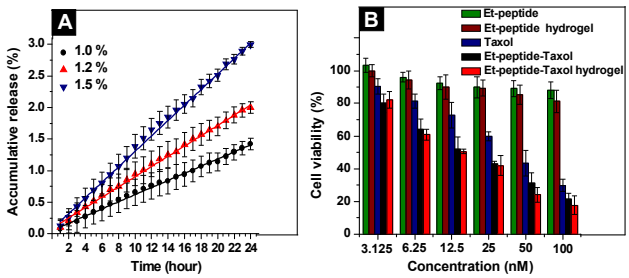

Fig.2 (A) Accumulative release profile of Taxol from different concentration (1.0, 1.2 and 1.5%) of hydrogels at 37°C in 0.1 M PBS solutions (pH7.4, n=3). **(B)** Cytotoxicity of Et-peptide (hydrogel), Taxol, and Et-peptide-Taxol (hydrogel) after incubated with MCF-7 cells for 48 h.

Indocyanine green (ICG) is the currently only U.S. Federal Drug Administration approved NIR clinical imaging agent and has been used in clinical for many decades as a contrast agent for retinal angiography and liver function studies.[26] ICG absorbs strongly and also fluoresces in the near-infrared region, to which biological tissue is relatively transparent. Therefore, we choose the ICG to conjugate with the hydrogels to perform imaging *in vivo* and *in vitro*. Compared to freely dissolved ICG, the emission spectrum of the ICG-peptide is red-shifted by from 790 to 802 nm and the fluorescence intensity had an apparent increase at this wavelength (Fig.S-4A). The red-shift of the fluorescence spectrum is explained by the partial delocalization of charge excitons into the new formed region.[27] Fluorescence intensity has an apparent increase at 802 nm was another evidence of the formation between ICG and peptide. It may be due to the noncovalent binding between ICG and peptide as a strong competition, which reduced the selfaggregation between ICG and ICG.[28] It is hypothesized that, due to the existence of –COOH and -NH_2, peptide contributes considerably to an increase in the vander Waals forces and electrostatic interactions.[29] The images of ICG have good monodispersity and bright red fluorescence (Fig. S-4B). When conjugate with the peptide and form the hydrogel, the formation exhibits filamentous structures (Fig.S-4C). This result is consistent with TEM images.

To visualize the subcellular localization and cellular uptake of hydrogel by confocal microscopy, MCF-7 cells were incubated with non-targeting, single-targeting and Et-peptide-Taxol hydrogels conjugated with fluorescence ICG for 4 h. Compared to non- and single-targeting hydrogels (Fig.S-5(a-f)), Et-peptide-Taxol hydrogel exhibits stronger fluorescence signal on the surface membrane of MCF-7 cells (Fig.S-5(g-i)), indicating that Et-peptide-Taxol is efficiently taken up by MCF-7 cells under the synergistic effect of both targeted estrone and RGD peptide. Meanwhile, the fluorescence is hardly observed from control SCG7901cells (Fig.S-5(j-l)) because there is absence of specific-targeted estrogen receptor on gastric cancer cells. The enhancement in targeting and binding imparted by hydrogel is likely due to differences in their ability to engage in binding with

estrone receptor and integrin $\alpha_v\beta_3$ on the surface of breast cancer cells. The results clearly demonstrate that dual-targeting of the peptide improve hydrogel binding its site of action and targeting drug delivery.

The fluorescence was visible in the cells as early as 4 h after incubation and began to visibly affect cells structure 12 h after treatment (Fig.3). By 12 h, cells treated with dual-targeting hydrogels begin to bleb, indicative of apoptosis, and the red fluorescence can be found in the cell cytoplasm and nucleus (Fig.3 (g-i)). In contrast, the MCF-7 cells treated with single-targeting hydrogel are bloat and abnormal (Fig.3 (d-f)), and that with non-targeting hydrogel remain almost intact (Fig.3 (a-c)). The survival time of MCF-7 cells after administering Et-peptide-Taxol hydrogel is significantly shorter than that of the non- and single-targeting hydrogels. Based on apoptosis assays, it can be concluded that the apoptosis and necrotic effect of the Taxol loaded hydrogels is markedly elevated by the dual-modification with estrone and RGD peptide.[30] Thus, it requires shorter time for the internalized hydrogels to release their cargo and nuclear accumulation of Taxol. The likely processes could be explained by the following three steps: (1) Estrone recognizes ER on the surface of cancer cells and binds with ER. (2) RGD peptide promotes the Et-peptide-Taxol to bind to integrin $\alpha_v\beta_3$. (3) After crossing cells membrane, The drug delivery penetrated cancer cells to release free Taxol. All these three steps are associated with the ER and integrin $\alpha_v\beta_3$ overexpression on breast cancer cells.

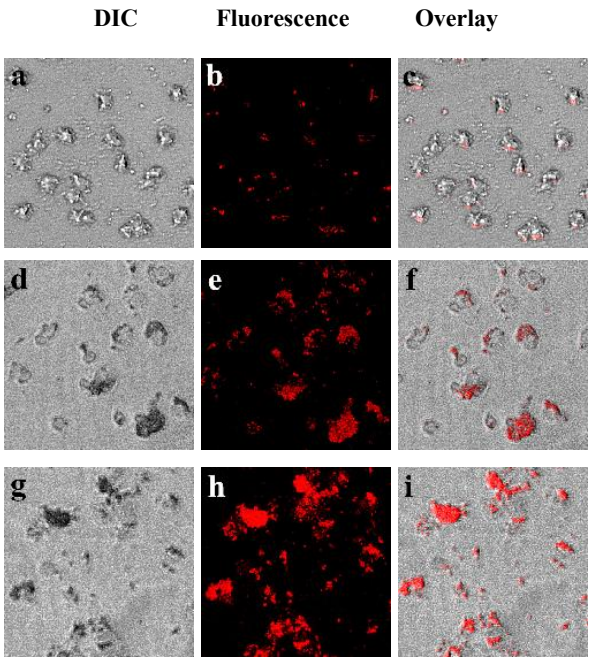

Fig.3 Confocal images of MCF-7 cells after incubation with non-targeting (a-c), single-targeting (d-f) and dual-targeting (g-i) hydrogels for 12 h after being washed by PBS solution (Bar: 100μm)

Time dependent biodistribution was studied by using a noninvasive near-infrared fluorescence imaging system (NIR). A series of *in vivo* images reflecting the bio-distribution of Et-peptide-Taxol hydrogel show the active tumor targeting mechanisms. Optical imaging data (Fig.4) suggest that, after intravenous tail vein injection of Et-peptide-Taxol hydrogel, fluorescence signal in nude mice has systemic distribution for a short time then accumulates together in the liver. After 30 min, a clearly visible fluorescence accumulates in the region of tumor. As time went on, the signal intensity obviously enhances and easily observes for 48 h. After 1 h from injection the signal enhancement in the bladder indicates the part of carrier is eliminated from body by urine excretion. From this time point, fluorescent signal is clearly monitored in the gastrointestinal part and last for a long time. As to the macromolecule and polar Et-peptide-Taxol hydrogel, the drug transforms into metabolites in the liver after intravenous injection. The metabolites are excreted into bile, and then eliminated into intestine. The drug transformed from metabolites is reabsorbed in intestine again. This process is called entero-hepatic cycle. With the passage of time the hydrogel except that accumulated in the region of tumor is almost eliminated from the body after 48 h. There is no death and side effect phenomenon to occur in the process of monitoring. Histopathology changes are investigated at the end of treatment after five days. No noticeable histopathology changes of vital tissues (heart, liver, spleen, lung and kidney) of mice are visually observed (Fig.S-6), but cells death is found in the tumor tissue. *In vivo* the distribution of Et-peptide-Taxol hydrogel shows the highest distribution selectively in the tumor region, which is contributed by the synergistic effect of estrone and RGD peptide. The results demonstrate that Et-peptide-Taxol hydrogel could not only selectively target the breast tumor but also easily metabolize to biocompatible materials.

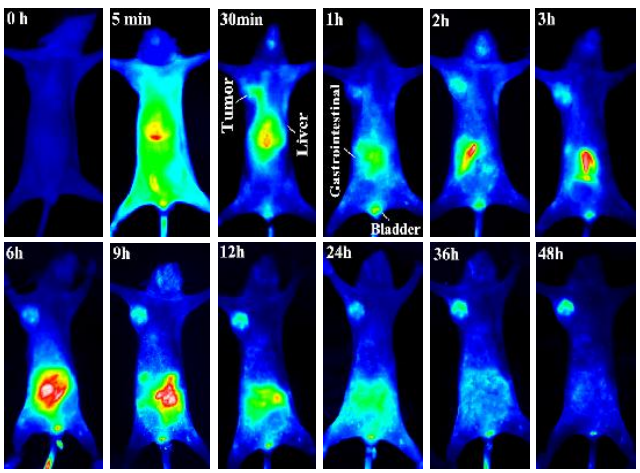

Fig.4 Optical images of a nude mice with tail vein injection of Et-peptide-Taxol hydrogel.

In the present study, we developed a novel dual-targeting hydrogel by conjugating with estrone and RGD peptide, which transported drugs, specific targeting tumor and penetrated breast cancer cells. The effects of peptide properties, morphology, stability and affinity on drug delivery and therapeutic efficacy were investigated. It did enhance the accumulation hydrogel within the cancer cells and breast tumor as evidenced *in vitro* confocal imaging and *in vivo* NIR. The present experimental data clearly show that estrone and RGD peptide as tumor-targeting moiety is responsible for a preferential accumulation of Et-peptide-Taxol hydrogel in the breast tumor, their effective

internalization by cancer cells and sustained release of the drug inside the cells. These findings demonstrate a biocompatible, sustained release, synergistic dual-targeting, highly anticancer efficient and novel route for anticancer agents to the breast cancer.

The authors gratefully acknowledge the financial support from the National Natural Science Foundation of China (No. 81173023) and the College Graduate Scientific Research and Innovation Program of JiangSu Province of China (No. KYLX_0616).

Notes and references

1. N. Stephanopoulos, J. H. Ortony and S. I. Stupp, *Acta Mater.*, 2013, **61**, 912-930.
2. J. Panyam and V. Labhasetwar, *Adv. Drug Deliver. Rev.*, 2012, **64, Supplement**, 61-71.
3. S. C. Lee, I. K. Kwon and K. Park, *Adv. Drug Deliver. Rev.*, 2013, **65**, 17-20.
4. C. Ren, Z. Song, W. Zheng, X. Chen, L. Wang, D. Kong and Z. Yang, *Chem. Commun.*, 2011, **47**, 1619-1621.
5. H. Wang, C. Yang, L. Wang, D. Kong, Y. Zhang and Z. Yang, *Chem. Comm.*, 2011, **47**, 4439-4441.
6. J. Li, Y. Gao, Y. Kuang, J. Shi, X. Du, J. Zhou, H. Wang, Z. Yang and B. Xu, *J. Am. Chem. Soc.*, 2013, **135**, 9907-9914.
7. Y. Gao, Y. Kuang, Z.-F. Guo, Z. Guo, I. J. Krauss and B. Xu, *J. Am. Chem. Soc.*, 2009, **131**, 13576-13577.
8. O. Cohen and R. Granek, *Nano Lett.*, 2014, **14**, 2515-2521.
9. J. Han, T. Lei and Q. Wu, *Carbohyd. Polym.*, 2014, **102**, 306-316.
10. B. B. Metaferia, M. Rittler, J. S. Gheeya, A. Lee, H. Hempel, A. Plaza, W. G. Stetler-Stevenson, C. A. Bewley and J. Khan, *Bioorg. Med. Chem. Let.*, 2010, **20**, 7337-7340.
11. D. G. Belair, A. S. Khalil, M. J. Miller and W. L. Murphy, *Biomacromolecules*, 2014, **15**, 2038-2048.
12. Q. Yang, K. Wang, J. Nie, B. Du and G. Tang, *Biomacromolecules*, 2014, **15**, 2285-2293.
13. P. E. Lønning, B. P. Haynes, A. H. Straume, A. Dunbier, H. Helle, S. Knappskog and M. Dowsett, *Steroids*, 2011, **76**, 786-791.
14. S. R. Paliwal, R. Paliwal, H. C. Pal, A. K. Saxena, P. R. Sharma, P. N. Gupta, G. P. Agrawal and S. P. Vyas, *Mol. Pharmaceutics*, 2011, **9**, 176-186.
15. H. Drzewiecka and P. P. Jagodzinski, *Biomed. Pharmacother.*, 2012, **66**, 530-534.
16. E. Shamaeli and N. Alizadeh, *Int. J. Pharm.*, 2014, **472**, 327-338.
17. H. A. Kim, K. Nam and S. W. Kim, *Biomaterials*, 2014, **35**, 7543-7552.
18. Y.-P. Yu, Q. Wang, Y.-C. Liu and Y. Xie, *Biomaterials*, 2014, **35**, 1667-1675.
19. J. B. Townsend, F. Shaheen, R. Liu and K. S. Lam, *J. Comb. Chem.*, 2010, **12**, 700-712.
20. X. Li, C. Yang, Z. Zhang, Z. Wu, Y. Deng, G. Liang, Z. Yang and H. Chen, *J. Mater. Chem.*, 2012, **22**, 21838-21840.
21. T. Doane and C. Burda, *Adv. Drug Deliver. Rev.*, 2013, **65**, 607-621.
22. P. L. P. Ritger, N. A., *J. Controlled Release*, 1987, **5**, 23-26.
23. H. Peng, W. Li, F. Ning, L. Yao, M. Luo, X. Zhu, Q. Zhao and H. Xiong, *J. Agric. Food Chem.*, 2013, **62**, 626-633.
24. S. Khansari, S. Duzyer, S. Sinha-Ray, A. Hockenberger, A. L. Yarin and B. Pourdeyhimi, *Mol. Pharmaceutics*, 2013, **10**, 4509-4526.
25. H. Wang, L. Lv, G. Xu, C. Yang, J. Sun and Z. Yang, *J. Mater. Chem.*, 2012, **22**, 16933-16938.
26. R. Watanabe, K. Sato, H. Hanaoka, T. Harada, T. Nakajima, I. Kim, C. H. Paik, A. M. Wu, P. L. Choyke and H. Kobayashi, *ACS Med.Chem. Lett.*, 2014, **5**, 411-415.
27. X. Zheng, D. Xing, F. Zhou, B. Wu and W. R. Chen, *Mol. Pharmaceutics*, 2011, **8**, 447-456.
28. X. Zheng, F. Zhou, B. Wu, W. R. Chen and D. Xing, *Mol. Pharmaceutics*, 2012, **9**, 514-522.
29. T. Zong, L. Mei, H. Gao, W. Cai, P. Zhu, K. Shi, J. Chen, Y. Wang, F. Gao and Q. He, *Mol. Pharmaceutics*, 2014.
30. A. O. Elzoghby, *J. Control. Release*, 2013, **172**, 1075-1091.

